

MODELING FUTURE URBAN GROWTH AND GREEN INFRASTRUCTURE INTEGRATION IN ILORIN METROPOLIS USING INTEGRATED CA-MARKOV AND GIS APPROACHES

*¹Ipadeola Oyedapo Ademuyiwa ²Babalola Ayo

¹⁻²Department of Surveying and Geoinformatics,
Faculty of Environmental Sciences
University of Ilorin, Nigeria.

¹<https://orcid.org/0000-0002-3-3900>

²<https://orcid.org/0000-0003-0129-1631>

*Corresponding Author's email: ipadeola.ao@unilorin.edu.ng

ABSTRACT

Rapid urbanization in sub-saharan Africa has led to profound land use and land cover (LULC) changes, posing significant challenges for environmental sustainability and urban resilience. This study investigates historical and projected LULC dynamics in Ilorin Metropolis, Nigeria, from 1990 to 2020, with projections for 2030 and 2040, emphasizing the integration of green infrastructure (GI) in urban land use. Multi-temporal satellite imagery classified through remote sensing and GIS methods quantified LULC changes, while a hybrid Cellular Automata-Markov (CA-Markov) model simulated future scenarios incorporating GI principles. Results showed a sharp increase in built-up areas from 7.78% (1990) to 39.64% (2020), primarily encroaching on vegetation and bare lands. Vegetation declined initially but exhibited partial recovery due to reforestation and GI initiatives. The CA-Markov model's accuracy ($\kappa > 0.8$) supports its application for planning transitions toward sustainable urban development. The findings highlight the urgent need to integrate GI elements such as urban green spaces, ecological corridors, and permeable surfaces into land use planning to mitigate environmental degradation, enhance ecosystem services, and improve urban livability in Ilorin and similar rapidly urbanizing African cities

KEYWORDS: Land Use/Land Cover Change, Urbanization, CA-Markov Modeling, Green infrastructure (GI), Remote Sensing

1. INTRODUCTION

Urbanization is a defining hallmark of the 21st century, driven by advances in science, technology, and societal capacity to transform natural environments (Liu, Pei, Wen, Li, Wang, Wu, Liu, 2019; Tirziu, 2020; Chen, Li, Liu, Chen, Liang, Leng, Huang, 2021; Long, Zhang, Ma, Tu, 2021; Mohanty & Kumar, 2021). While crucial for modernization and economic growth, rapid urbanization poses significant challenges to environmental sustainability, especially in rapidly developing regions such as Sub-Saharan Africa (Agyemang & Silva, 2019; Auwalu & Bello, 2023; Patel & Raval, 2024). Ecological sustainability entails meeting present needs without compromising ecosystem health for future generations (Emina, 2021; Hariram, Mekha, Suganthan, & Sudhakar, 2023).

Urbanization remains a major driver reshaping global landscapes, often outpacing planning and regulatory capacities and causing serious environmental stress (Seto, Güneralp, & Hutyrá, 2012; Chen *et al.*, 2021). Conventional urban growth has prioritized built-up land expansion at the expense of green cover, resulting in habitat fragmentation, biodiversity loss, and degraded ecosystem services. Green infrastructure (GI), a planned network of natural and semi-natural spaces including parks, green corridors, and wetlands, offers a sustainable alternative by conserving biodiversity, regulating microclimates, improving air quality, and mitigating stormwater impacts (Liang, Du, Wang, & Xu, 2020; Pandey & Ghosh, 2023).

In rapidly urbanizing cities like Ilorin Metropolis, Nigeria, unplanned sprawl has converted extensive vegetation and agricultural lands into built environments, exacerbating urban heat islands, surface runoff, and pollution. Integrating GI into urban land use planning is a promising approach to foster multifunctional green spaces that benefit both ecological integrity and human well-being (Mohamed, Worku, & Lika, 2020; Ait El Haj Fatiha, Ouadif Latifa, & Akhssas Ahmed, 2023). This study applies advanced remote sensing, GIS, and hybrid Cellular Automata-Markov (CA-Markov) modeling to analyze historical trends and project future land use/land cover (LULC) patterns, explicitly considering GI to guide sustainable urban growth and environmental resilience in Ilorin.

Land use planning balances social, economic, and environmental objectives by allocating land purposefully to guide development and reduce negative impacts (Cobbinah, Poku-Boansi, & Peprah, 2017; Mohamed *et al.*, 2020; Liang *et al.*, 2020; Solly, 2021; Kalfas, Kalogiannidis, Chatzitheodoridis, & Toska, 2023). Yet, global urban land expanded from 274,700 km² in 1992 to 621,100 km² in 2016 and is projected to more than double by 2030 (He, Li, & Liu, 2019; Seto *et al.*, 2012). This growth is particularly pronounced in Sub-Saharan Africa, where urban land increased over threefold from 7,700 km² in 1992 to 27,600 km² in 2016, with projections suggesting a twelvefold rise between 2000 and 2050 (Angel, Parent, Civco, Blei, & Potere, 2011). Unplanned expansion has led to loss of fertile soils, habitats, and green spaces, significantly impacting biodiversity and ecosystem services (Tope-Ajayi, 2016; Sumari, Cobbinah, Ujoh, & Xu, 2020; Mohammadyari *et al.*, 2023). Studies from cities such as Abuja, Morogoro, Mafikeng, and Rundu report comparable vegetation and agricultural land loss, while planning effectiveness suffers due to limited data, inadequate assessments, and weak implementation (Mwathunga & Donaldson, 2018; Munyati & Drummond, 2020).

Accurate, timely LULC data underpins monitoring and sustainable policy-making (Gaur & Singh, 2023; Karimi & Sultana, 2024). Advances in satellite remote sensing and GIS enable robust multi-temporal change detection using platforms such as Landsat, MODIS, SAR, and CBERS. Analytical models Markov chains, cellular automata, and hybrid CA-Markov, offer powerful frameworks to simulate urban growth and environmental impacts (Wu & Ma, 2019; Mostafa, Li, & Sadek, 2023; Mirzakhani, Behzadfar, & Azizi Habashi, 2025). Hybrid CA-Markov models improve prediction by integrating spatial and temporal dynamics, proving invaluable for scenario analysis and sustainable planning incorporating GI principles (Ait El Haj Fatiha *et al*, 2023; Agyemang, Silva, & Fox, 2023).

Ilorin exemplifies rapid urbanization typical of emerging African cities, with widespread conversion of fertile lands and green cover to built-up areas. This unregulated growth has caused habitat destruction, pollution, soil erosion, increased runoff, urban heat islands, and elevated greenhouse gas emissions, threatening environmental sustainability and human health (Ipadeola, Odunaiya, Tella, Issa, Yusuf, & Olabode, 2018; Idrees, Adepoju, Ipadeola, Omar, Alade, & Salami, 2021). Integrating GI into urban planning offers a strategic pathway to mitigate these impacts by preserving and enhancing ecosystem functions within the urban fabric.

This research monitors LULC changes in Ilorin from 1990 to 2020 to model future urban growth and green infrastructure integration dynamics in the Ilorin metropolis using integrated CA-markov and GIS approaches. Objectives include producing classified LULC maps, calculating land consumption rates and absorption coefficients, and deriving transition matrices to model land use dynamics. Emphasizing GI integration, the study provides scientific insights to support sustainable urban development and informed policymaking in Ilorin and similar Sub-Saharan African cities.

2. MATERIALS AND METHODS

2.1 Study Area

The research is conducted in Ilorin Metropolis, the capital of Kwara State, North-Central Nigeria (8°31'N, 4°35'E), and covered approximately 100 km². The city's flat terrain, bounded by the Asa and Oyun rivers, and its status as a major administrative and economic center have contributed to significant land transformation in recent decades. Ilorin's population is on the increase and experiencing rapid urban expansion and making it an ideal case for land use/land cover (LULC) dynamics research. The city's expansion has led to significant changes in land use patterns, with implications for environmental sustainability and public health (Ipadeola *et al*, 2018; Idrees *et al*, 2021). The study area map is presented in figure 1.

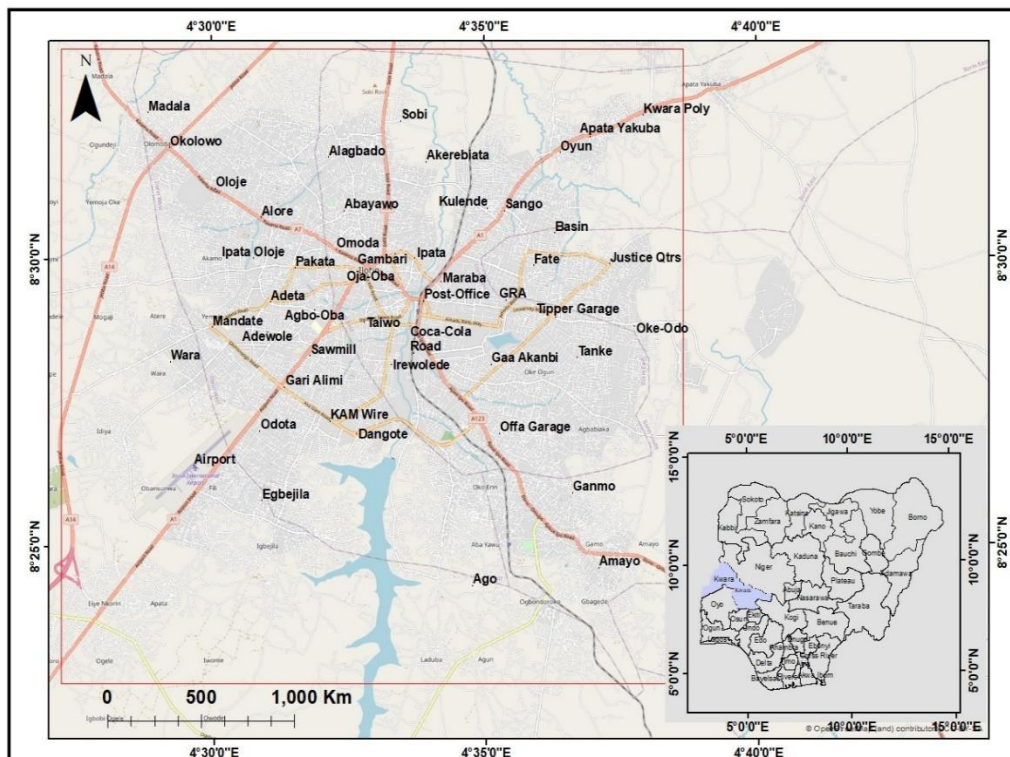


Figure 1: Study area map

2.2 Data Acquisition

2.2.1 Satellite Imagery

Four multi-temporal satellite images were acquired to analyze LULC dynamics at decadal intervals: Landsat Thematic Mapper (TM) for 1990, Landsat Enhanced Thematic Mapper Plus (ETM+) for 2000, Landsat Operational Land Imager/Thermal Infrared Sensor (OLI/TIRS) for 2015 and 2020. All images were sourced from the United States Geological Survey (USGS) Earth Explorer, with a spatial resolution of 30 meters. The selection of imagery prioritized cloud-free scenes and consistent seasonal periods to minimize phenological and atmospheric discrepancies (Jensen, 2015; Kollert, Bremer, Löw, & Rutzinger, 2021; Aravena, Lyons, & Keith, 2023). The satellite datasets used and their attributes are presented in Table 1.

Table 1: Satellite datasets used and their attributes.

S/N	Image	Date	Path/Row	Spectral bands	Cloud	LULC name	Zone	Spectral resolution
1	Landsat 5	1990/01/02	190/054	Bands 1,2,3,4	TM	LULC 1990	31N	30*30
2	Landsat 7	2000/11/13	190/054	Bands 1,2,3,4	ETM+	LULC 2000	31N	30*30
3	Landsat 8	2015/11/09	190/054	Bands 2,3,4,5	ETM+	LULC 2015	31N	30*30
4	Landsat 8	2020/11/28	190/054	Bands 2,3,4,5	OLI	LULC 2020	31N	30*30

2.2.2 Ancillary Data

Ancillary data used include the topographic maps and administrative boundaries for Ilorin Metropolis, the population data from the National Population Commission, other governmental sources, and Field data for ground truthing and accuracy assessment (Subramaniam, 2020; Aduloju, Anofi, Atolagbe, Raheem, & Ade, 2025).

2.2.3 Software and Tools Used

The software and tools used in the study included ERDAS Imagine, ArcGIS, and QGIS for remote sensing and GIS processing, particularly for image processing, classification, and spatial analysis. For modeling, IDRISI/TerrSet was employed to perform CA-Markov simulations. Statistical analysis involved the use of Microsoft Excel and R to conduct quantitative analyses of Landscape Change Rate (LCR), Landscape Aggregation Index (LAC), and transition probabilities. Additionally, ArcGIS and QGIS were utilized for spatial visualization and map production (Subramaniam, 2020).

2.3 Data Processing

2.3.1 Image Preprocessing

To ensure the reliability and comparability of the satellite data, several preprocessing steps were implemented. Radiometric correction was applied to adjust for sensor noise and atmospheric interference (Jin, Ahn, Seo, & Choi, 2020). Geometric correction involved georeferencing all images to the Universal Transverse Mercator (UTM) projection, Zone 31N, using the WGS 84 datum (Jensen, 2015). Additionally, subsetting and cloud masking were performed by clipping the images to the study area boundary and identifying cloud and shadow pixels, which were excluded from the analysis through thresholding and manual editing (Kollert *et al.*, 2021).

2.3.2 Land Use/Land Cover Classification

Classification Scheme

A supervised classification approach was adopted, with the following LULC broad classes: Built-up Area, Vegetation, Water bodies, and bare land. The classification scheme was adapted from previous studies in Sub-Saharan Africa (Sumari, *et al.*, 2020; Govender, Dube, & Shoko, 2022), and also by us conducting a random field survey throughout the various neighborhoods. These observations were utilized to classify and map the four broad land cover types used. The input bands used in the study to produce false-colour composite maps consisted of bands 4, 3, and 2 for Landsat 5 TM and 7 ETM+, and bands 5, 4, and 3 for Landsat 8 OLI. The spectral signature of each image pixel was matched with the training samples of the study area, and the satellite images were classified into four broad land use/land cover (LULC) types.

Classification Method

Training Samples: Representative training samples for each class were collected using field surveys, high-resolution Google Earth imagery, and expert knowledge (Congalton & Green, 2019; Shetty, Gupta, Belgiu, & Srivastav, 2021).

Algorithm: The Maximum Likelihood Classification (MLC) algorithm was applied due to its effectiveness in handling multispectral data and its widespread acceptance in LULC studies (Jensen, 2015; Congalton & Green, 2019).

Post-Classification Smoothing: A 3x3 majority filter was applied to reduce classification noise (Paluba, Papale, Perivolioti, Stych, Laštovička, Kalaitzis, ... & Mouratidis, 2023).

2.3.3 Accuracy Assessment

Accuracy was evaluated using a confusion matrix and the kappa coefficient, with independent validation points. The overall accuracy (OA) measures the proportion of correctly classified pixels, while the kappa coefficient (K) adjusts for chance agreement, ranging from -1 to 1. A kappa value above 0.85 indicates almost perfect agreement and is considered acceptable for further analysis (Owoeye & Ibitoye, 2016; Congalton & Green, 2019; Dettori & Norvell, 2020). This rigorous assessment ensures high reliability and validity in the LULC classification results, supporting robust change detection and modeling.

$$\text{Overall Accuracy (OA)} = \left[\frac{(Pc) + (Nc)}{(Pc) + (Fp) + (Nc) + (Fn)} \right] \times 100 \dots \text{eqn. (1)}$$

$$\text{Kappa coefficient (K)} = \frac{OA - P(e)}{1 - P(e)} \dots \text{eqn. (2)}$$

Where OA denotes overall accuracy and the percentage of correctly classified cases. Pc is the proportion of correctly identified positive cases. Nc denotes the number of correctly classified negative cases. Fp denotes the number of incorrectly classified negative cases as positive. Fn is the number of positive cases that were incorrectly classified as unfavourable. P (e) is defined as the expected ratio by chance (i.e., the proportion of the sum of marginal probabilities multiplication by the class to the total class entries).

2.4 Change Detection and Quantitative Analysis

2.4.1 Land Consumption Rate (LCR) and Land Absorption Coefficient (LAC)

The LCR and LAC for the research were computed using the processed data results. LCR is calculated as the ratio of the increase in built-up area to the corresponding population growth over each period, and LAC is determined as the rate of built-up area expansion per year. The formula for the land consumption rate and absorption coefficient is given below.

$$\text{Land consumption rate (LCR)} = \frac{A}{P} \dots \text{eqn. (3)}$$

A = the city's area in hectares, P = the population

$$\text{Land absorption coefficient (LAC)} = \frac{A_2 - A_1}{P_2 - P_1} \dots\dots\dots \text{eqn. (4)}$$

P_1 and P_2 are the population figures for the early and later years, respectively. A_1 and A_2 are the areas extended (in hectares) for the early and later years (Idrees *et al.*, 2021)

LCR is the measure of a study area's progressive spatial urbanisation, and LAC is the measure of change in urban land by each unit increase in urban population (Ipadeola *et al.*, 2018); 1990, 2000, 2015, and 2020 population figures of the study area were estimated from the 2006 census using the recommended National Population Commission (NPC) 2.6% growth rate as obtained from Nigeria population growth rate 2006 (Idrees *et al.*, 2021). This is represented by equations (5) and (6).

$$n = \frac{r}{100} \times P_0 \dots\dots\dots \text{eqn. (5)}$$

$$P_n = P_0 + (n \times t) \dots\dots\dots \text{eqn. (6)}$$

P_n = estimated population (2000, 2017), P_0 = base year population (2006 population figure), r = growth rate (2.1%), n = annual population growth, t = number of years projected.

2.5 Post-Classification Comparison (PCC)

The post-classification comparison (PCC) method was used to quantify LULC transitions in Ilorin by independently classifying multi-temporal satellite images (1990, 2000, 2015, and 2020) and overlaying them in GIS to generate cross-tabulation matrices. This enabled precise pixel-level tracking of land cover changes, identification of transition hotspots, and calculation of gains, losses, and net changes for each class. Statistical and graphical analyses, supported by high classification accuracy ($\text{kappa} > 0.82$), provided a robust and reliable framework for monitoring and understanding LULC dynamics over the study period (Verma, Raghubanshi, Srivastava, & Raghubanshi, 2020; Alemu, Warkineh, Lulekal, & Asfaw, 2024).

2.6 LULC Change Simulation and Projection

The hybrid Cellular Automata-Markov (CA-Markov) model was employed to project Ilorin's LULC patterns for 2030 and 2040 by integrating the spatial dynamics of cellular automata with the temporal transition probabilities of the Markov chain (Eastman, 2016; Wu & Ma, 2019; Mondal, Sharma, Kappas, & Garg, 2020). This approach overcomes the limitations of single models by simulating both the likelihood and spatial patterns of land cover change. Using classified LULC maps from multiple periods, transition probability and area matrices, and suitability maps for key classes, the model was implemented in IDRISI-TerrSet with a 5x5 contiguity filter to enhance spatial realism. Calibration and validation against observed data yielded high kappa agreement ($\text{kappa} > 0.8$), confirming the model's reliability. The validated 2020 LULC map was then used to forecast land cover for 2030 and 2040, providing robust, spatially explicit projections for urban planning.

$$L_{(x+1)} = P_{ij} \times L_{(x)} \dots\dots\dots \text{Eqn (7)}$$

The transition probabilities are calculated from the transition samples that occur during a specific time interval and displayed in the transition matrix (P).

$$P_{ij} = \begin{bmatrix} P_{11} & P_{12} & P_{13} & \dots & P_{1m} & P_{21} & P_{22} & P_{23} & \dots & P_{2m} & P_{31} & P_{32} & P_{33} & \dots & \dots & \dots & P_{3m} & P_{mm} \end{bmatrix} \dots \dots \dots \text{Eqn (8)}$$

Where $L_{(x+1)}$ and $L_{(x)}$ are the land use/land cover conditions at time (x+1) and (x), respectively. $0 \leq P_{ij} < 1$ and $\sum_j^m P_{ij} = 1, P_{ij} = 1, (i,j = 1,2,3,\dots,m)$ is the transition probability matrix.

This hybrid CA-Markov approach effectively captures both temporal transition dynamics and spatial dependencies, making it a powerful tool for simulating future LULC scenarios to support sustainable land management and urban planning (Mondal *et al.*, 2020; Ait El Haj Fatiha *et al.*, 2023).

3.0 RESULTS AND DISCUSSION

3.1 Land Use/Land Cover (LULC) Change Dynamics (1990–2020)

LULC Distribution and Trends

The classified LULC maps for Ilorin Metropolis for the years 1990, 2000, 2015, and 2020 revealed significant spatial and quantitative transformations (Table 2; Figure 2). Over the past 30 years, built-up areas expanded markedly, primarily at the expense of vegetation and agricultural land.

Table 2: LULC Area Statistics (1990–2020)

LULC TYPES	1990 (Sq Km)	%	2000 (Sq Km)	%	2015 (Sq Km)	%	2020 (Sq Km)	%
Water bodies	401.94	1.22	381.51	1.16	386.73	1.18	394.74	1.20
Built-up/urban	2554.74	7.78	3541.77	10.78	8891.55	27.07	13020.30	39.64
Vegetation	4424.13	13.47	12457.35	37.93	2385.54	7.26	3578.04	10.90
Bare ground	25462.89	77.53	16463.07	50.13	21179.88	64.49	15850.62	48.26
Total area	32,843.70		32,843.70		32,843.70		32,843.70	
		100		100		100		100

Built-up Area: The built-up area in Ilorin Metropolis experienced a substantial and continuous increase over the study period. Between 1990 and 2020, the proportion of land classified as built-up increased from 7.78% to 39.64% representing a net growth of approximately 31.86 percentage points over the period and a more than fourfold rise. The most rapid expansion occurred between 2015 and 2020, highlighting the city’s accelerated urbanization.

The CA-Markov projection indicates that built-up areas will likely reach 51.7% by 2030 and 63.4% by 2040 if current trends persist. This rapid expansion reflects the intense urbanization and population growth in Ilorin, which saw its population rise from 515,000 in 1990 to 950,000 in 2020. The spatial pattern of growth is characterized by outward expansion from the city center, often following major road corridors and encroaching on peri-urban lands. Notably, the

development pattern includes leapfrogging, where new urban areas bypass vacant lands closer to the core, leading to fragmented urban landscapes. This unplanned and sprawling growth undermines land use planning efforts and increases the cost of infrastructure and service provision (Agyemang *et al.*, 2023).

Vegetation: Vegetation cover fluctuated, rising from 13.47% in 1990 to 34.11% in 2000, then sharply declining to 7.29% in 2015, before partially recovering to 10.90% in 2020. Overall, this indicates a decrease of 2.57% points between 1990 and 2020. The model projects a further reduction to 11.2% by 2030 and only 6.8% by 2040. The loss of vegetation is primarily due to conversion for urban development and, to a lesser extent, agricultural expansion. This decline threatens local biodiversity, disrupts ecosystem services, and exacerbates urban heat island effects and air quality issues (Tope-Ajayi, 2016; Pandey & Ghosh, 2023). The reduction in vegetative cover also increases vulnerability to soil erosion, surface runoff, and flooding, especially in areas near the Asa and Oyun rivers. The observed trend is consistent with findings in other Sub-Saharan African cities, where urban expansion has led to significant green space degradation (Sumari *et al.*, 2020).

Bare Land: Bare land showed a general decline, starting at 77.53% (25,462.89 sq km) in 1990, dropping to 48.26% (15,850.62 sq km) in 2020, a reduction of 29.27%. This reflects the conversion of open land to urban and, to a lesser extent, vegetated uses.

Water Bodies: Water bodies remained relatively stable, fluctuating slightly between 1.22% in 1990 to 1.20% in 2020. While water bodies have not been directly affected by urban expansion to the same extent as vegetation, the encroachment of built-up areas near riverbanks and floodplains poses risks for water quality and flood regulation. The stability of water bodies may mask underlying threats such as pollution, siltation, and reduced ecosystem function due to surrounding land use changes. The preservation of riparian buffers and the enforcement of setback regulations are critical for maintaining the ecological integrity of these water resources. Spatial analysis shows that urban expansion radiated outward from the city center, following major transportation corridors and encroaching on peri-urban agricultural and vegetated areas. The expansion pattern is characteristic of leapfrogging and sprawl, with new developments bypassing vacant lands closer to the urban core. Figure 2 presents the spatial pattern of the land use land cover dynamics of the metropolis between 1990 and 2020.

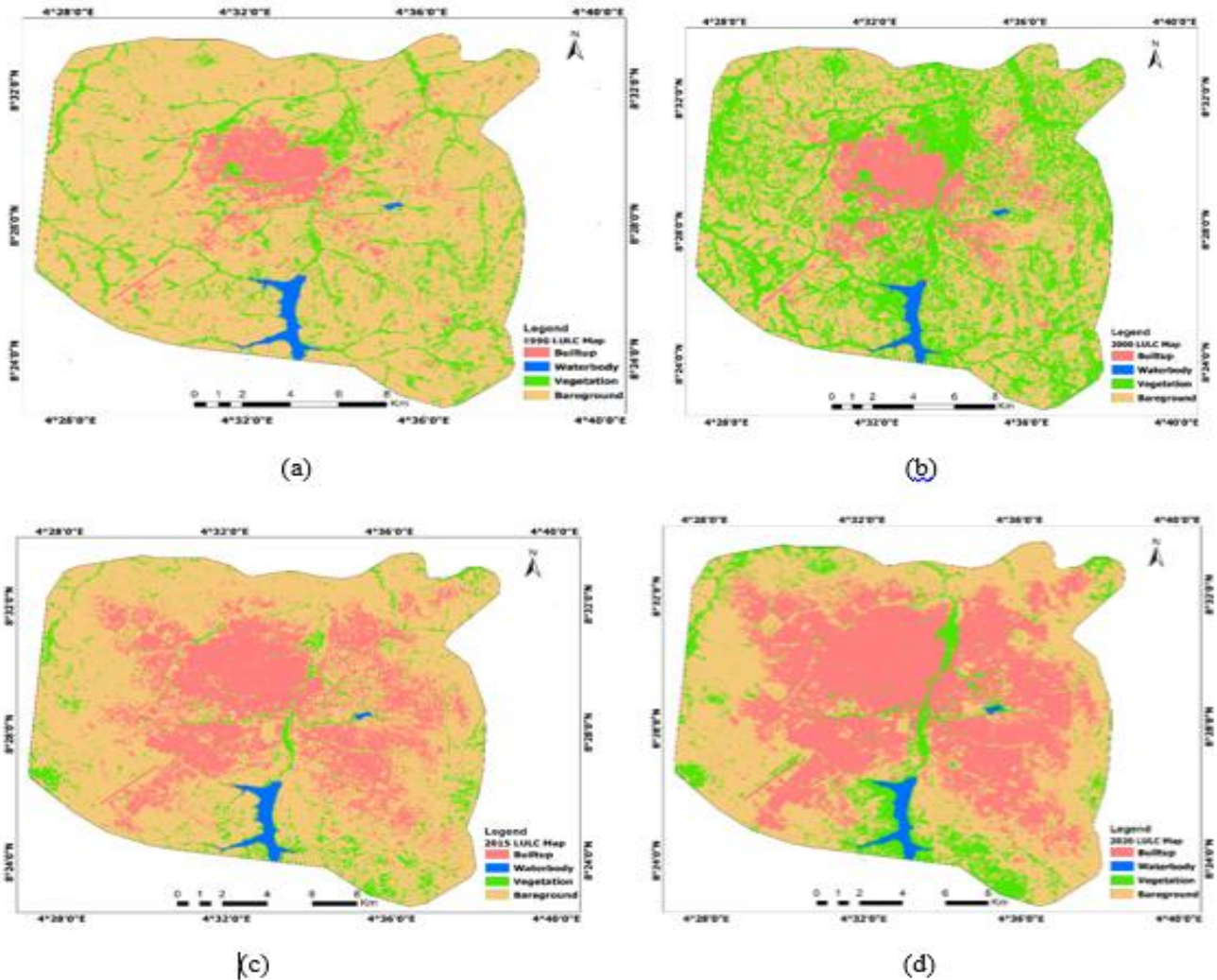


Figure 2: Classified land use/land cover (LULC) of Ilorin Metropolis in 1990 (a), 2000 (b), 2015 (c), and 2020 (d)

3.2 Land Consumption Rate and Land Absorption Coefficient

The Land Consumption Rate (LCR) and Land Absorption Coefficient (LAC) were computed to quantify the efficiency and intensity of land conversion. LCR peaked at 0.028 km²/person during the 2015–2020 period, reflecting increased land uptake per capita due to inefficient land use and low-density development. LAC increased steadily, indicating a growing annual rate of built-up area expansion. These metrics underscore the unsustainable trajectory of urban growth, with implications for resource use and environmental integrity. Table 3 and figure 3 present the losses, gains, and net changes of LULC classes for the periods between 1990 and 2020.

Table 3: Losses, gains, and net changes of LULC classes for the periods between 1990 and 2020 (In hectares)

LULC change types	Losses	Gains	Net change
WATERBODIES	22.59	15.39	-7.20
BUILT-UP/URBAN	188.46	10654.02	10465.56
VEGETATION	3386.70	2540.61	-846.09
BARE GROUND	12034.08	2421.81	-9612.27

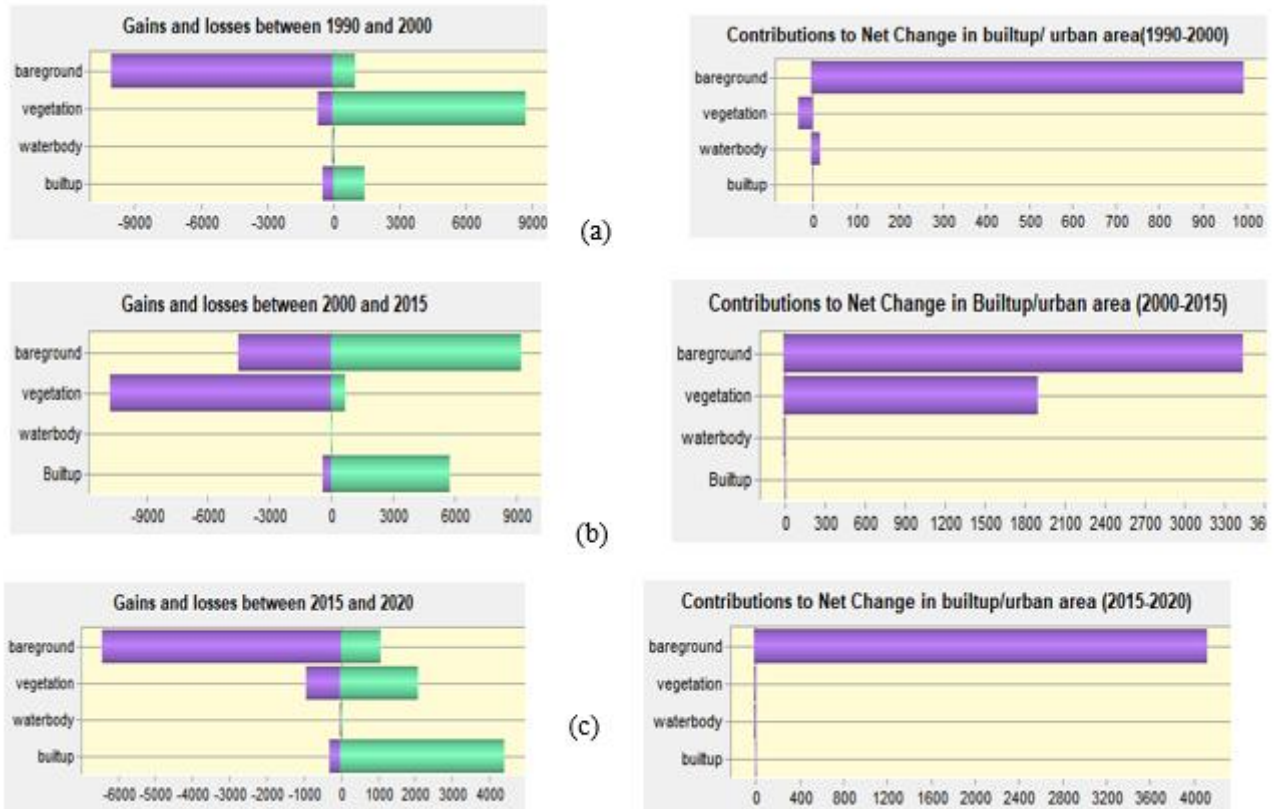


Figure 3: Losses and gains in LULC (in hectares) and net change contributions to built-up areas in hectares between (a) 1990-2000, (b) 2000-2015, and (c) 2015-2020

3.3 Assessment of Classification Accuracy

The kappa coefficients and total accuracies for all the classified LULC maps of 1990, 2000, and 2020 were above 80% and 0.75, as shown in Table 4. This demonstrates a dependable and accurate image classification for analyzing land use/land cover change.

Table 4: Assessment of classification accuracy

S/No	LULC Types	1990		2000		2020	
		Producer's Accuracy	User's Accuracy	Producer's Accuracy	User's accuracy	Producer's accuracy	User's accuracy
1.	Built-up area	81.28	100.00	78.84	88.17	86.16	100.00
2.	Vegetation	86.63	71.07	85.89	84.08	80.76	77.81
3.	Barren land	86.50	86.77	95.40	86.64	96.02	86.13
4.	Water bodies	81.69	91.98	69.41	90.77	94.44	100.00
5.	Overall accuracy	84.39%		86.48%		88.50%	
6.	Overall kappa	0.79		0.80		0.84	

3.4 Markov Transition Matrix Analysis

The Markov transition matrix reveals a rising likelihood of barren land and water bodies being converted to built-up areas, increasing from 3.0% and 0.8% (1990–2000) to 12.57% and 1.17% (2015–2020) (Table 5), respectively, driven by rapid urban growth and population pressure. The probability of barren land and water bodies transitioning to vegetation also increased significantly, reflecting agricultural and irrigation initiatives. Meanwhile, the chance of vegetation changing to built-up areas grew from 3.4% to 4.1%, highlighting ongoing urban expansion and the need for scenario-based LULC monitoring.

Table 5: Markov probability matrix for LULC change during the periods from 2000 to 2015 and 2015 to 2020

Year (Period)	LULC Classes	Built-Up Area	Vegetation	bare ground	Water Bodies
2000–2015 (Period 1)	Built-up area	0.9484	0.0000	0.0503	0.0012
	Water bodies	0.0059	0.0009	0.0000	0.9932
	vegetation	0.0123	0.2364	0.7514	0.0000
	bare ground	0.1057	0.0438	0.8505	0.0000
2015–2020 (Period 2)	Built-up area	0.8989	0.0220	0.0730	0.0061
	waterbodies	0.0113	0.0623	0.0394	0.8870
	vegetation	0.3172	0.2331	0.4483	0.0015
	bare ground	0.5207	0.1244	0.3527	0.0022

3.5 Summary of CA–Markov Simulation Results and Implications (2020–2040)

The CA–Markov model's validation produced strong kappa statistics ($K_{no} = 0.7698$, $K_{location} = 0.8336$, $K_{locationStrat} = 0.8336$, $K_{standard} = 0.6997$), indicating good agreement between predicted and observed land cover, and confirming the model's reliability for future LULC simulations. Based on this, the classified 2020 LULC map, along with transition probability and area matrices from 2015–2020, was used to forecast Ilorin's land cover for 2030 and 2040. The resulting projections, detailed in Table 6 and illustrated in Figures 4 and 5, provide a robust basis for understanding and managing future land cover dynamics in the metropolis.

Table 6: Statistical distribution of the modelled LULC in 2030 and 2040

Year/Period	2020		2030		2040		LULC Change 2020 – 2030		LULC Change 2020 – 2040	
	Area (Ha)	Area (%)	Area (Ha)	Area (%)	Area (Ha)	Area (%)	Area (Ha)	Area (%)	Area (Ha)	Area (%)
Land Use/Land Cover Classes										
Built-up area	13,020.30	39.64	18,152.10	55.27	21,172.95	64.47	5,131.80	15.63	8,152.65	24.83
Vegetation	3578.04	10.90	3683.52	11.22	3116.88	9.49	105.48	0.32	-461.16	-1.41
bare ground	15,850.62	48.26	10,630.26	32.37	8,180.55	24.91	-5220.36	-15.89	-7,670.07	-23.35
Water bodies	394.74	1.20	377.82	1.15	373.32	1.14	-16.92	-0.05	-21.42	-0.06
Total	32,843.70	100	32,843.70	100	32,843.70	100	-	-	-	-

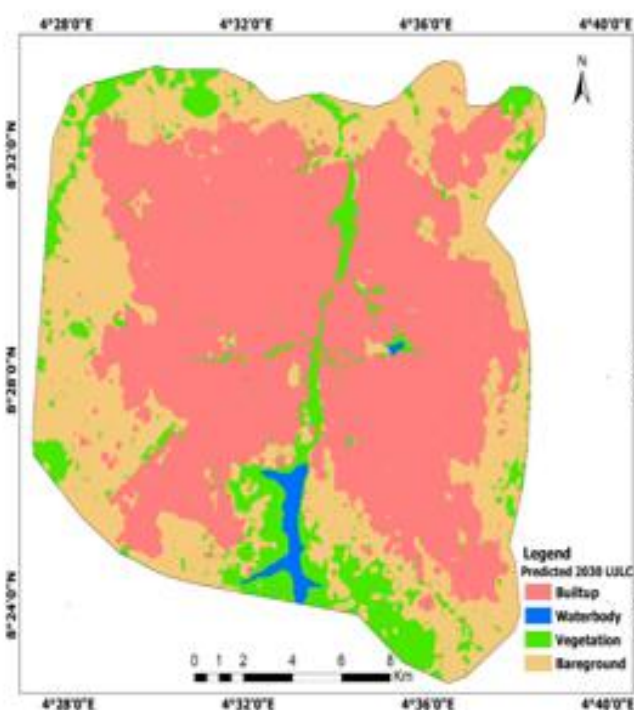


Figure 4 Modelled 2030 LULC map of Ilorin Metropolis.

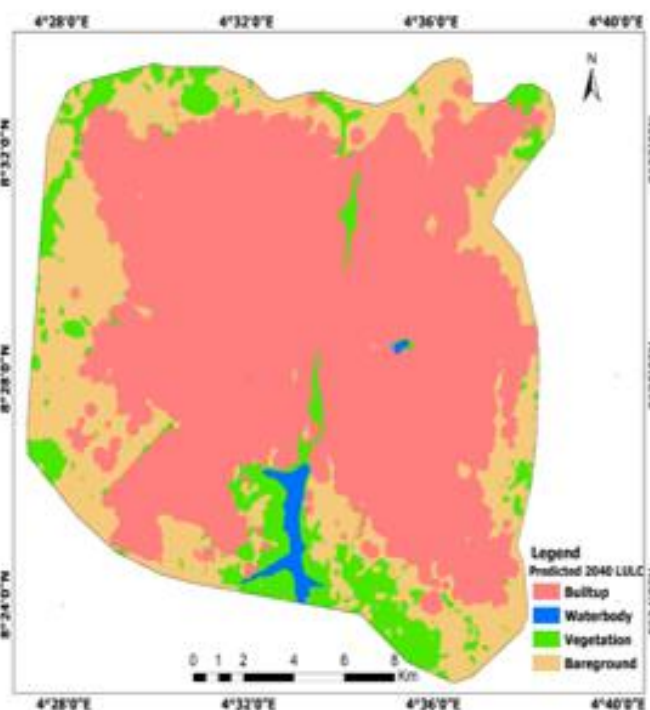


Figure 5 Modelled 2040 LULC map of Ilorin Metropolis

The CA–Markov model predicts that Ilorin’s built-up area will grow significantly from 13,020.30 ha in 2020 to about 18,152.10 ha in 2030 and 21,172.95 ha by 2040, driven by ongoing urbanization and socio-economic activities. Vegetation cover is projected to rise slightly to 3,683.52 ha by 2030 but decline to 3,116.88 ha by 2040, reflecting both reforestation efforts and continued urban encroachment. Barren land will decrease markedly from 15,850.62 ha in

2020 to 10,630.26 ha in 2030 and 8,180.55 ha in 2040, while water bodies will remain relatively stable with a slight decrease. These trends highlight the city's dynamic land cover transitions, largely influenced by population growth, infrastructure development, and agricultural expansion. The findings align with previous studies that link urban growth to socio-economic and biophysical drivers, emphasizing the need for balanced policies. Without effective urban planning and environmental safeguards, continued expansion threatens agricultural land, natural habitats, and sustainable development. Policymakers must prioritize integrated land management strategies to harmonize urban growth with ecological preservation in Ilorin Metropolis.

3.6 Summary of Implications

The analysis confirmed extensive urban growth in Ilorin Metropolis from 1990 to 2020, with built-up areas expanding from 7.78% to 39.64%, primarily replacing vegetated and bare lands. Vegetation cover, a vital component of green infrastructure (GI), showed fluctuations with partial recovery in later years due to reforestation efforts, highlighting the potential of GI adoption to mitigate the adverse effects of unplanned expansion. CA-Markov projections suggest that without enhanced GI integration, urban areas could occupy over 60% of the land by 2040, intensifying pressure on ecological systems.

These findings underscore the critical role of GI in urban planning to counterbalance green space loss, reduce urban heat island effects, improve stormwater management, and conserve biodiversity (Pandey & Ghosh, 2023; Mohamed et al., 2020). The observed diffusion and leapfrogging urban expansion patterns highlight the necessity of strategically establishing GI networks to maintain landscape connectivity and ecosystem services within Ilorin's evolving urban fabric. The rapid, largely unplanned urbanization mirrors trends across Sub-Saharan Africa, where weak planning and enforcement have failed to safeguard environmentally sensitive areas (Mohamed et al., 2020; Agyemang et al., 2023).

Environmental consequences include biodiversity loss and habitat fragmentation, increased flood risk and surface runoff from impermeable surfaces, food security challenges due to shrinking agricultural lands, exacerbated urban heat islands, and declining air quality from reduced vegetation. Urgent integrated land use planning, strengthened environmental regulation enforcement, sustainable urban development practices, real-time geospatial monitoring, active stakeholder engagement, and establishment of urban greenbelts are vital to mitigating unplanned growth impacts and fostering a resilient, sustainable future for Ilorin Metropolis.

4. CONCLUSION

This study reveals that Ilorin Metropolis has undergone rapid and unsustainable land use/land cover (LULC) changes from 1990 to 2020, with built-up areas expanding by 416% and vegetation declining by 83.7%, trends projected to continue through 2040. Urban expansion, driven by population growth and uncoordinated development, has largely replaced vegetated and agricultural lands, resulting in biodiversity loss, increased surface runoff, urban heat islands, and threats to food security. Despite existing land use plans, weak implementation has allowed haphazard growth and leapfrogging into sensitive areas, heightening ecological risks. The CA-Markov model captured these spatial dynamics, highlighting ongoing degradation without intervention. Utilizing integrated remote sensing, GIS, and CA-Markov approaches, this research provides robust, data-driven insights to monitor urban growth and guide effective planning. Crucially, the findings stress that Ilorin's urbanization is unsustainable under current frameworks

and emphasize the urgent need to integrate green infrastructure into land use strategies to promote resilient and environmentally sustainable metropolitan development.

5. RECOMMENDATIONS

To promote sustainable urban development and environmental management in Ilorin Metropolis, it is essential to strengthen integrated land use planning supported by robust legal frameworks and effective enforcement mechanisms that protect and expand urban green spaces, ecological corridors, and riparian buffers (Kalfas et al., 2023; Ait El Haj Fatiha et al., 2023). Incorporating green infrastructure (GI) suitability criteria within spatial planning and CA-Markov modeling tools will facilitate balanced land use decisions that harmonize urban growth with ecological preservation. Establishing and legally safeguarding greenbelts and ecological corridors, particularly near water bodies, alongside continuous remote sensing and GIS-based monitoring, will enable proactive management of land cover changes and enhance GI effectiveness in mitigating urbanization impacts (Agyemang & Silva, 2019; Mohamed et al., 2020). Additionally, fostering inclusive participatory planning processes by engaging local communities, civil society, and the private sector is vital to build capacity among planners and environmental managers. Improving access to reliable spatial data and geospatial tools will empower informed decision-making. Together, these measures will balance development with environmental stewardship, promoting long-term urban resilience and improving residents' well-being.

REFERENCES

- Aduloju, O. T., Anofi, A. O., Atolagbe, A. A., Raheem, W. M., & Ade, M. A. (2025). Space-Time Estimation of Built-Up Landscape of Ilorin Metropolis, Nigeria. *Papers in Applied Geography*, 1-24.
- Agyemang, F. S., & Silva, E. (2019). Simulating the urban growth of a predominantly informal Ghanaian city-region with a cellular automata model: Implications for urban planning and policy. *Applied Geography*, 105, 15-24.
- Agyemang, F. S., Silva, E., & Fox, S. (2023). Modelling and simulating 'informal urbanization': An integrated agent-based and cellular automata model of urban residential growth in Ghana. *Environment and Planning B: Urban Analytics and City Science*, 50(4), 863-877.
- Ait El Haj Fatiha, Ouadif Latifa, Akhssas Ahmed. (2023). Simulating and predicting future land-use/land cover trends using CA-Markov and LCM models. *ScienceDirect*.
- Akintunde, J. A. (2016). Spatio-temporal pattern of urban growth in Jos Metropolis, Nigeria. *Remote Sensing Applications: Society and Environment*, 4, 44-54.
- Aldana-Domínguez, J. P.-A.-S. (2019). Assessing the effects of past and future land cover changes in ecosystem services, disservices, and biodiversity: A case study in Barranquilla Metropolitan Area (BMA), Colombia. *Ecosystem Services*, 37, 100915.
- Alemu, M., Warkineh, B., Lulekal, E., & Asfaw, Z. (2024). Analysis of land use land cover change dynamics in Habru District, Amhara Region, Ethiopia. *Heliyon*, 10(19).
- Angel, S., Parent, J., Civco, D. L., Blei, A., & Potere, D. (2011). The dimensions of global urban expansion: Estimates and projections for all countries, 2000-2050. *Progress in Planning*, 75(2), 53-107.

- Auwalu, F. K., & Bello, M. (2023). Exploring the contemporary challenges of urbanization and the role of sustainable urban development: a study of Lagos City, Nigeria. *Journal of Contemporary Urban Affairs*, 7(1), 175-188.
- Aravena, R. A., Lyons, M. B., & Keith, D. A. (2023). High resolution forest masking for seasonal monitoring with a regionalized and colourimetrically assisted chorologic typology. *Remote Sensing*, 15(14), 3457.
- Chen, G., Li, X., Liu, X., Chen, Y., Liang, X., Leng, J., ... & Huang, K. (2020). Global projections of future urban land expansion under shared socioeconomic pathways. *Nature Communications*, 11(1), 537.
- Cobbinah, P. B., Poku-Boansi, M., & Peprah, C. (2017). Urban environmental problems in Ghana. *Environmental Development*, 23, 33-46.
- Congalton, R. G., & Green, K. (2019). *Assessing the Accuracy of Remotely Sensed Data*.
- Dettori, J. R., & Norvell, D. C. (2020). Kappa and beyond: is there agreement? *Global Spine Journal*, 10(4), 499-501.
- Eastman, J. R. (2016). *TerrSet Geospatial Monitoring and Modeling System Manual*.
- Emina, K. A. (2021). Sustainable development and the future generations. *Social Sciences, Humanities and Education Journal (SHE Journal)*, 2(1), 57-71.
- Gaur, S., & Singh, R. (2023). A comprehensive review on land use/land cover (LULC) change modeling for urban development: Current status and prospects. *Sustainability*, 15(2), 903.
- Govender, T., Dube, T., & Shoko, C. (2022). Remote sensing of land use-land cover change and climate variability on hydrological processes in Sub-Saharan Africa: Key scientific strides and challenges. *Geocarto International*, 37(25), 10925-10949.
- Hariram, N. P., Mekha, K. B., Suganthan, V., & Sudhakar, K. (2023). Sustainalism: An integrated socio-economic-environmental model to address sustainable development and sustainability. *Sustainability*, 15(13), 10682.
- He, C., Li, X., & Liu, Z. (2019). Detecting global urban expansion over the last three decades using a fully convolutional network. *Environmental Research Letters*, 14(3), 034008.
- Idrees, M. O., Adepoju, B. D., Ipadeola, A. O., Omar, D. M., Alade, A. K., & Salami, I. B. (2021). Evaluating urban sprawl and land consumption rate in Ilorin metropolis using multitemporal landsat imagery. *Environmental Technology and Science Journal*, 12(2), 37-47.
- Ipadeola, A. O., Odunaiya, A. K., Tella, A. K., Issa, B. S., Yusuf, A., & Olabode, T. B. (2018). Geospatial analysis of the land use and land cover changes of Ilorin metropolis between 2000 and 2017 using remote sensing and GIS techniques.
- Jensen, J. R. (2015). *Introductory Digital Image Processing: A Remote Sensing Perspective* (4th ed.). Pearson.
- Jin, C., Ahn, H., Seo, D., & Choi, C. (2020). Radiometric Calibration and Uncertainty Analysis of KOMPSAT-3A Using the Reflectance-Based Method. *Sensors*, 20(9), 2564.
- Kalfas, D., Kalogiannidis, S., Chatzitheodoridis, F., & Toska, E. (2023). Urbanization and land use planning for achieving the sustainable development goals (SDGs): A case study of Greece. *Urban Science*, 7(2), 43.
- Karimi, F., & Sultana, S. (2024). Urban expansion prediction and land use/land cover change modeling for sustainable urban development. *Sustainability*, 16(6), 2285.
- Kollert, A., Bremer, M., Löw, M., & Rutzinger, M. (2021). Exploring the potential of land surface phenology and seasonal cloud free composites of one year of Sentinel-2 imagery

- for tree species mapping in a mountainous region. *International Journal of Applied Earth Observation and Geoinformation*, 94, 102208.
- Liang, Y., Du, M., Wang, X., & Xu, X. (2020). Planning for urban life: A new approach of sustainable land use plan based on transit-oriented development. *Evaluation and Program Planning*, 80, 101811.
- Long, H., Zhang, Y., Ma, L., & Tu, S. (2021). Land use transitions: Progress, challenges and prospects. *Land*, 10(9), 903.
- Liu, X., Pei, F., Wen, Y., Li, X., Wang, S., Wu, C., ... & Liu, Z. (2019). Global urban expansion offsets climate-driven increases in terrestrial net primary productivity. *Nature Communications*, 10(1), 5558.
- Mirzakhani, A., Behzadfar, M., & Azizi Habashi, S. (2025). Simulating urban expansion dynamics in Tehran through satellite imagery and cellular automata Markov chain modelling. *Modeling Earth Systems and Environment*, 11(2), 145.
- Mohamed, A., Worku, H., & Lika, T. (2020). Urban and regional planning approaches for sustainable governance: The case of Addis Ababa and the surrounding area changing landscape. *City and Environment Interactions*, 8, 100050.
- Mohammadyari, F., Zarandian, A., Mirsanjari, M. M., Suziedelyte Visockiene, J., & Tumeliene, E. (2023). Modelling impact of urban expansion on ecosystem services: a scenario-based approach in a mixed natural/urbanised landscape. *Land*, 12(2), 291.
- Mohanty, R., & Kumar, B. P. (2021). Urbanization and smart cities. In *Solving urban infrastructure problems using smart city technologies* (pp. 143-158). Elsevier.
- Mondal, M. S., Sharma, N., Kappas, M., & Garg, P. K. (2020). CA Markov modeling of land use land cover change predictions and effect of numerical iterations, image interval on prediction results. *ISPRS Archives*, XLIII-B3, 713-720.
- Mostafa, E., Li, X., & Sadek, M. (2023). Urbanization trends analysis using hybrid modeling of fuzzy analytical hierarchical process-cellular automata-Markov chain and investigating its impact on land surface temperature over Gharbia City, Egypt. *Remote Sensing*, 15(3), 843.
- Munyati, C., & Drummond, J. H. (2020). Loss of urban green spaces in Mafikeng, South Africa. *World Development Perspectives*, 19, 100226.
- Mwathunga, E., & Donaldson, R. (2018). Urban land contestations, challenges and planning strategies in Malawi's main urban centres. *Land Use Policy*, 77, 1-8.
- Owoeye, J. O., & Ibitoye, O. A. (2016). Analysis of Akure urban land use change detection from remote imagery perspective. *Urban Studies Research*, 2016(1), 4673019.
- Paluba, D., Papale, L. G., Perivolioti, T. M., Štych, P., Laštovička, J., Kalaitzis, P., ... & Mouratidis, A. (2023). Unsupervised burned area mapping in Greece: Investigating the impact of precipitation, pre-and post-processing of Sentinel-1 data in Google Earth Engine. In *IGARSS 2023-2023 IEEE International Geoscience and Remote Sensing Symposium* (pp. 2520-2523). IEEE.
- Pandey, B., & Ghosh, A. (2023). Urban ecosystem services and climate change: a dynamic interplay. *Frontiers in Sustainable Cities*, 5, 1281430.
- Patel, J. B., & Raval, Z. (2024). The impacts of urbanization on ecological systems: a comprehensive study of the complex challenges arising from rapid urban growth. *Research Review Journal of Indian Knowledge Systems*, 1(1), 1-10.

- Seto, K. C., Güneralp, B., & Hutyra, L. R. (2012). Global forecasts of urban expansion to 2030 and direct impacts on biodiversity and carbon pools. *Proceedings of the National Academy of Sciences*, 109(40), 16083-16088.
- Shetty, S., Gupta, P. K., Belgiu, M., & Srivastav, S. K. (2021). Assessing the effect of training sampling design on the performance of machine learning classifiers for land cover mapping using multi-temporal remote sensing data and Google Earth Engine. *Remote Sensing*, 13(8), 1433.
- Solly, A. (2021). Land use challenges, sustainability and the spatial planning balancing act: Insights from Sweden and Switzerland. *European Planning Studies*, 29(4), 637-653.
- Subramaniam, L. M. (2020). LandMet: landscape metrics tool in QGIS to study landscape variability (Master's thesis, New Mexico State University).
- Sumari, N. S., Cobbinah, P. B., Ujoh, F., & Xu, G. (2020). On the absurdity of rapid urbanization: Spatio-temporal analysis of land-use changes in Morogoro, Tanzania. *Cities*, 107, 102876.
- Tirziu, A. M. (2020). Urbanization and cities of the future. *International Journal for Innovation Education and Research*, 8(3), 235-245.
- Tope-Ajayi, O. O. (2016). Land Use Change Assessment, Prediction Using Remote Sensing, and GIS Aided Markov Chain Modelling at Eleyele Wetland Area, Nigeria. *Journal of Settlements and Spatial Planning*, 7(1), 51-63.
- Verma, P., Raghubanshi, A., Srivastava, P. K., & Raghubanshi, A. S. (2020). Appraisal of kappa-based metrics and disagreement indices of accuracy assessment for parametric and nonparametric techniques used in LULC classification and change detection. *Modeling Earth Systems and Environment*, 6(2), 1045-1059.
- Wu, Y., & Ma, L. (2019). Environmental evaluation in strategic planning. *Journal of Environmental Management*, 232, 1022-1031.